

Information Transmission Concept Based Model of Wave Propagation in Discrete Excitable Media

Š. Raudys

Institute of Mathematics and Informatics
Akademijos st. 4, 08663 Vilnius, Lithuania
raudys@ktl.mii.lt

Received: 26.05.2004

Accepted: 02.07.2004

Abstract. A new information transmission concept based model of excitable media with continuous outputs of the model's cells and variable excitation time is proposed. Continuous character of the outputs instigates infinitesimal inaccuracies in calculations. It generates countless number of the cells' excitation variants that occur in front of the wave even in the homogenous and isotropic grid. New approach allows obtain many wave propagation patterns observed in real world experiments and known simulation studies. The model suggests a new spiral breakup mechanism based on tensions and gradually deepening clefts that appear in front of the wave caused by uneven propagation speed of curved and planar segments of the wave. The analysis hints that the wave breakdown and daughter wavelet bursting behavior possibly is inherent peculiarity of excitable media with weak ties between the cells, short refractory period and granular structure. The model suggested is located between cellular automaton with discrete outputs and differential equation based models and gives a new tool to simulate wave propagation patterns in applied disciplines. It is also a new line of attack aimed to understand wave bursting, propagation and annihilation processes in isotropic homogenous media.

Keywords: arrhythmia, bursting, cellular automatons, chaos, daughter wavelets, spirals, wave breakdown.

1 Introduction

Excitable media are spatially distributed systems which have the ability to propagate signals without damping. Such system can be considered as a group of

individual elements tied to each other. Each element can transfer the information to its neighbors. A signal over a certain threshold initiates a wave of activity moving across the excitable media [1, 2]. Traveling waves have been observed in autocatalytic chemical reactions, biological cells and tissues, ecology, meteorology, cosmology and seismology [2]–[8]. In real world applications, computer simulations and experiments performed *in numero* can yield information that cannot be obtained in any other way [9].

Despite the obvious differences, signal propagation in all excitable media share many characteristics. Underlying mathematical modes to analyze excitable media in chemistry and biological tissues are systems of differential equations and cellular automata (CA) [1, 3, 5, 9, 10]. Helpful systematization of physical phenomena as well as computerized numerical models of the wave propagation, uniform and turbulent wave processes in excitable media have been presented in monograph [3] and especially in Chapter 12 written by Winfree. Good review of modern cellular automaton based models is presented in Gil Bub thesis [2].

Mathematical models of excitable media can be formulated as systems of differential equations or finite difference equations which characterize the rate of change of certain variables over the time. Differential equations are valid in absolutely homogeneous media. Very popular are Fitzhugh-Nagumo dynamics and Hodgkin-Huxley [9, 10] systems of differential equations originally suggested to analyze a quantitative description of the membrane current in nerve.

Accurate simulation of traveling waves becomes computationally expensive as complexity of the underlying models increases. If a large number of spatially discrete points are required, simulations may require a prohibitive amount of computer time [9, 11]. In addition, the variables of the model are mutually dependent. Changing one variable can change more than one characteristic of the model. Therefore, complex models are not appropriate for generating all-purpose results applicable to all excitable media. Moreover, real media is not homogeneous. Therefore, often excitable media is simulated using discrete time models, called cellular automata [1, 11]. These models consist of a grid of nodes. In first models, each element in the node (cell) could exist in one of three states: resting, excited or refractory. There is a set of rules that determine future states of the cells in the grid based on the present state of the grid. A resting cell updates

its state in reliance on the activity of its neighbors. The excited and refractory cells renew their state based on the element's history. A resting cell remains at rest until a certain number of neighboring cells become excited. In such case, the cell becomes excited in the next time moment. The excited cells become refractory and the refractory cells return to rest. Thus, cellular automaton models simplify the dynamic description of a system by mapping the systems behavior onto a few discrete states. It is a level of abstraction over differential equations as a number of underlying variables are encompassed into a single state. They are more intuitively transparent and computer simulations run far faster. The simplicity of cellular automata makes them popular as models for physical and biological systems [1, 2].

Cellular automata research in excitable media was first investigated in a biological context by Wiener and Rosenblueth [6], who modeled waves rotating around the obstacles in models of excitable cardiac muscle. The first computer simulations were performed by Farley [12], who laid out virtual neural network (NN) on the rectangular grid, utilized 0 or 1 outputs of each cell and measured a time in periodic time moments. Moe, Rheinbolt and Abildskov [13], Balakhovskij [14], Krinsky [15], Greenberg and Hastings [16] developed the CA approach further. In later research, models where a number of excited states are greater than one and more than one neighbor must be active in order to induce a resting cell to the excited state were developed. A weighing function where cell's relative contribution to excitability decreases as a function of distance from the wave front and the relative refractory period (where cells have a higher threshold than resting cells but can still be excited) were introduced. Gerhardt and colleagues [11, 17] make an excitation threshold a decreasing function of time. Marcus and Hess [18] and Kurrer and Schulten [19] randomize the grid in circular or square neighborhoods. To diminish difference between the differential equations and cellular automata approaches continuous differential equation models began to be used in each element of the CA grid [2, 20, 21].

Differential equations and cellular automata methodologies allow to model a number of signal propagation patterns observed experimentally in various real excitable media: regular uniform of wave propagation outwards from a center of starting excitation, spiral waves (rotors) generation after their initiation, or

hitting the wave a non-conductive obstacle, disorganized activity, broken waves propagation in one or several directions, annihilations of two colliding waves and their breakdown as they reach border of excitable media or near a tip of the spiral. It was found that wave propagation speed depends on recovery time of the medium. The speed near the spiral tip is influenced by a shape of the tip and excitability of the media. The wave speed depends on a curvature of the wave front. Relationships between spiral core size and period for stationary spirals were established analytically [22]. A number of realistic 2D and 3D models that explain regular and chaotic phenomena in chemical reactions and mammalian heart were developed [8].

Nevertheless, in spite of great number of CA and differential equation based models a number of important questions remain to be unsolved. Practical applications of wave research have had little therapeutic impact to date in the arrhythmia problems [23]. Most of the spiral solutions assume that excitation occurs much faster than recovery, which is not valid in real systems [11]. In synthetic models, the spiral birth are caused only by specially planned artificial excitations [24]–[26], assigning a random probability for non refractory grid points to fire output signal [1, 2], a presence of non-conductive obstacles, non-homogeneities in refractory period, the excitation threshold or conductance of excitable media [6, 7, 27]. In practice, however, spontaneous birth and termination of spiral waves was observed. Mechanisms of wave bursting and break up, however, is not well understood [23, 28, 29].

One of possible ways to increase explanation of numerous experimental observations of the wave propagation patterns is utilization of different model types to simulate the same behavior of the wave initiation, propagation and breakdown. Possibly, a large number of models could suggest diverse mechanisms of these phenomena. Another way is to develop models that are intermediate between CA and differential equation based models.

Characteristic peculiarity of excitable media is that, not the physical signal, however, the information transmitted from one media element to other ones is very important. *An objective of present paper* is to consider the wave initiation, propagation and breakdown from a point of view of information transmission. Granular artificial neural network [30] based models will be considered. Contrary

to standard CA approach with discrete outputs of the automaton, we utilize single layer perceptron (SLP) with smooth sigmoid function that gives continuous outputs.

The SLP is the nature inspired model of information processing and transmission. Continuous cells' outputs, varying magnitudes of the weights (connection strengths between the neurons) used to calculate weighted sums of several adjacent cells, the smooth activation function award the SLP certain universality properties [31]. Only in a limit where the weights are large, the activation function saturates and begins to behave like a discrete threshold function with outputs 0 and 1. Theory shows that magnitudes of the weights are very important in defining properties of classification and prediction rules obtained while training the SLP [32]–[34]. An increase in perceptron weights also affects the networks ability to learn new information [35]. Encouraged by these findings I tried not to move away too far from basic neuron model in constructing cellular models of excitable media. One of important particularities of present analysis is utilization of very simple idealized 2D models that assume *a homogeneous and isotropic medium*.

The paper is organized as follows. In the second section 2D cellular media model is introduced and used to analyze stimulus propagation. In third section I analyze an influence of the magnitude of the weights, refractory period and other media's parameters. New explanation of the curvature effect, spontaneous wave birth, development of the wave fronts and breakdown in isotropic homogenous grid is suggested. The fourth section summarizes the model and its features.

2 Two dimensional excitable media model

Basic model of CA consist of a grid of nodes spaced on a regular grid. In new model, each element (cell) in the node is represented by the SLP. Cell-cell interaction is limited to adjacent neighbors. The SLP has a number (say p) of inputs x_1, x_2, \dots, x_p , one output o and performs operation $o = f(arg)$, where $arg = \sum_{i=1}^p w_i x_i$ is a weighted sum of inputs, and w_1, w_2, \dots, w_p are the weights (connection strengths between the cells).

In isotropic excitable media model, the weights are equal among themselves, i.e. $w_1 = w_2 = \dots = w_p = w$. In anisotropic model some of the weights can

differ. Here coefficient (weights) w_j determines the connection strength between s -th node and its neighbor in j -th direction. It is assumed that bilateral connection strengths are equal. In the hexagonal model, $p = 6$. It means that each cell transfer their output signals to six neighboring ones. Exceptions are cells on a boundary of the grid. Activation (transfer) function, $f(arg)$, is a non-linear soft-limiting transfer function which saturates at its both ends. We will make use of sigmoid function $f(arg) = 1/(1 + \exp(-arg))$ habitually utilized in artificial neural network studies. This function is bounded from underneath and on topside: it is equal or close to zero if the weighted sum, arg , is strongly negative, and is close to 1 if this sum is large positive.

The non-linear character and saturation of activation function are very important elements of the mathematical model. To make use of this model to simulate and analyze signal propagation in excitable media, we assume that arg can take only *positive values*. For this purpose a number of alternatives of the function were considered. In this paper we report results obtained with utilization of following function:

$$f(arg) = \begin{cases} \alpha/(1 + \exp(-\beta \times arg - \gamma)) - \eta & \text{if } arg \geq \Delta^*, \\ 0 & \text{otherwise} \end{cases} \quad (1)$$

where $\Delta^* \geq 0$ is a **sensitivity threshold**.

Constants $\alpha = 1.333$, $\beta = 5$, $\gamma = 0.4$ and $\eta = -1.333$ were selected specially to have the weights w varying between 0 and 1. Then, we have simple interpretation of the transfer strength, w . This function gives the output signal almost zero if argument, arg , is small and $\Delta^* = 0$. We have the output signal close to 1, if the weighted sum arg is large (Fig. 1). Following observations from physics and biology a sensitivity threshold Δ^* is introduced which gives an additional handle that can help to control the wave propagation process. In excitable media model, output signal from the s -th element, $o_s = f(arg_s)$, is multiplied by weight w_s and after time moment, t_{transf} , products $o_s \times w_s$ ($s = 1, \dots, p$) are transmitted to p neighbors. In new model the signal transmission time depends on strength of output signal, o . To define t_{transf} , we followed observations of Spach [36, 37]: “the longer is delay in transfer of the depolarization phase of the action potential across the gap junction, the greater the cell-to-cell charge transferred via the gap junction”. Similar observations can be found in chemistry (see e.g.

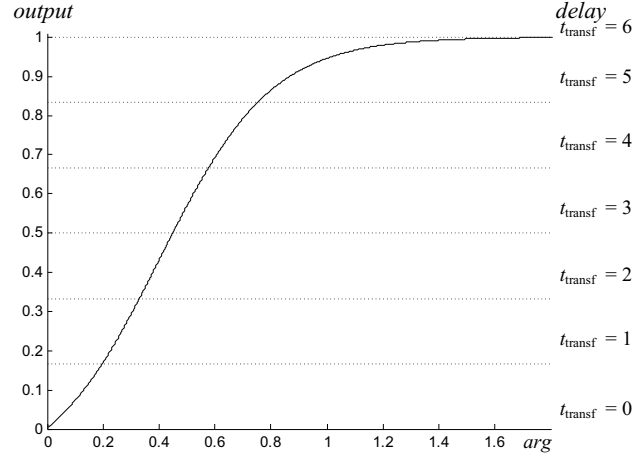


Fig. 1. Dependence of output and delay in firing output signal on input, weighted sum arg .

Chapter 13 written by Bowers and Noyes in [3]). Therefore, in new media model, we assume that the cell discharges its output signal after certain time period that is proportional to output signal, $f(arg)$. This particularity indicates that we have a “negative feed-back”: *the larger is excitation signal, arg , the later the cell will fire out its output signal, o* . In cellular automata models, signal transfer time, t_{transf} , is discrete. Therefore, the cell’s output signal $o = 1$ corresponds to maximal delay in effective transmission time, m . The output’s signal interval $(0, 1)$ is split into m equal intervals, corresponding to time moments $0, 1, 2, \dots, m-1$. Minimal transmission time is equal to 1, i.e. the cell does not transmit signal if $f(arg) < 1/m$. Minimal transmission time may be affected also by Δ^* . Discrete time measured in signal propagation steps and *proportionality of the time delay to the strength of the signal* are important elements of the model. The experiments showed that utilization of other schema (fixed or negative) of the time delay, t_{transf} , on output, o , changes the characteristics of the model essentially. Direct dependence, however, allows obtain many of the wave propagation patterns described in the literature. To speed up the calculations maximal interval of variations of cell inputs $(0, p)$ was split into $1000 \times p$ values and a look-up table was used to find $o = f(arg)$. The look-up table produces one more additional stochastic component.

An important parameter traditionally used in all cellular excitable media models is the refractory period, t_{refr} , a time when after excitation, the cell in the node cannot be excited. After the refractory period ends, the node can be excited again. In order expose all features of the media model with continuous outputs and varying signal transmission time, we considered *a priori fixed absolute refractory period*, t_{refr} , purposefully. In this paper we did not consider presence of relative refractory period.

Below we enumerate parameters used to determine the model:

- p_x and p_y , dimensions of 2D model,
- p , a number of neighbors, and the grid's shape,
- w_1, w_2, \dots, w_p , the connection weights,
- concrete parameters of transfer function $o = f(arg)$,
- Δ^* , sensitivity threshold,
- arg_{start} , starting excitation, and position of starting cell (or cells) in the grid,
- m , maximal delay in effective signal transmission time,
- t_{refr} , refractory period,
- a rule used to determine excitation time, t_{transf} .

Contrary to a large number of ionic currents, typically utilized in differential equations based models of biologic tissues, the parameters enumerated above have clearer interpretation for a layman.

Illustration. In Fig. 2 we depicted first 14 steps of wave propagation in a hexagonal homogeneous media model composed of 11×7 elements with $w = 0.72$. A central node, S , on bottom border (marked by “star”) is excited. In this and other experiments reported in this paper, $arg_{\text{start}} = 0.744$ and excitation of the starting cell (or cells) is performed only once. After four time moments ($t_{\text{transf}} = 4$) the starting cell, S , fires its output signal $o = f(0.744) = 0.8279$. This signal is transmitted to four neighbor cells, $\alpha, \beta, \gamma, \eta$, marked by “points”. All four cells are exited at the same time moment by signals of the same strength, $o \times w = 0.8279 \times 0.72 = 0.5961$. After next four time steps, cells $\alpha, \beta, \gamma, \eta$ fire out their output signals $o = f(0.596) = 0.6909$. These signals excite simultaneously seven neighboring nodes marked by “pluses”. Four nodes out of seven new ones are excited by single neighboring cells. Three cells, A, B and C, however, are excited by outputs of two adjacent cells (excitation is marked by

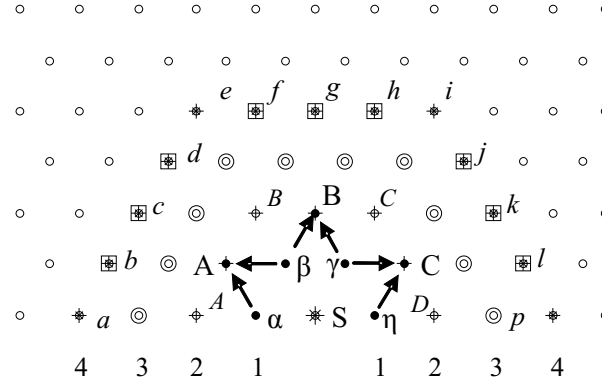


Fig. 2. First 14 time steps of signal transmission in hexagonal grid composed of 11×7 nodes.

arrows in Fig. 2) and accumulate double starting excitation, $arg = 2 \times 0.6909 \times 0.72 = 0.9949$. Each of remaining four cells are excited by one single cell, $arg = 0.6909 \times 0.72 = 0.4974$. It means that the three cells (A, B and C) *fire out their excitation after five time moments* ($t_{\text{transf}} = 5$), *and remaining four ones* (A, B, C, D) – *earlier, after three time moments* ($t_{\text{transf}} = 3$). Thus, the four nodes mentioned excite ten neighboring cells marked by “circle” simultaneously. These ten cells fire their outputs simultaneously after next two time moments and become refractory. Thus, outputs of cells A, B and C were outflowed by neighboring ones. This time, the outputs of cells A, B and C did not affect neighboring cells. The ten next cells (marked by circles) excite 13 following cells (a, b, \dots, l, p) after two time moments. Four cells, a, e, i and p , are excited by outputs of the single cells and fire their outputs just after one time moment ($t_{\text{transf}} = 1$). Each of remaining nine cells, b, c, d, f, g, h, j, k , and l (marked by “pluses” and “squares”) get their excitation from two neighboring cells and produce their outputs later, after four time moments.

This example illustrates that in the simplest hexagonal homogeneous media model, just at the very start we already can have *a vast variety of variants* of the nodes’ excitation times and the signal strengths. With an increase in radius of the wave, a number of the variants are increasing. Additional stochastic components are introduced by the inaccuracies caused by the calculations, organizing the

cycles in computer calculations, utilization of the look-up tables to determine outputs, $o = f(arg)$, and the cells' firing out time moments.

3 Signal propagation in homogeneous 2D media

3.1 Irregular propagation speed and the curvature effect

Summation of continuous cells' outputs, nonlinearity of the transfer function, $o = f(arg)$, and dependence of firing out time on the cell's excitation strength are very important differences of new cellular excitable media model in comparison with known ones. Information transmission principle based approach allows obtain many wave propagation patterns observed in real world experiments and simulation studies: single, letter "ω" shaped and multi-armed spirals initiated by temporary obstacles, non-homogeneities in conduction strengths, refractory period, wave breakup, e.t.c. Our main concern is elucidation of wave propagation mechanisms that cause spontaneous birth, development and breakdown of traveling waves.

The illustration in Fig. 2 shows that in direction of the angles of the hexagonal fragment of the grid, only *one cell* transmits its excitation further. On a straight line between the angles of hexagonal figure, *two cells* affect an unexcited cell ahead of the wave front. Dependence of the excitation time on the strength of output signal (Fig. 1) causes that signal propagation time along the angle of hexagonal figure should be higher as on the line connecting two angles. Consider the model with $w = 0.95$ and $m = 6$. Let the cells' output be $o = 0.9$. Since $m = 6$, it fires its output signal after $t_{\text{transf}} = 5$ time moments irrespective was this cell excited by one or by the two cells. If $w = 0.72$, the cell fires its output after $t_{\text{transf}} = 3$ time moments if it was excited by one cell. If this cell was excited by two neighboring cells, then the signal transmission time $t_{\text{transf}} = 4$. In this way, the differences in the wave propagation speed along diverse directions cause a curvature effect.

Fig. 3ab demonstrates *the curvature effect* in isotropic hexagonal model. Here a number of cells, S , situated on a straight line, was excited at the start. We see the wave fronts (just excited cells are marked by bold points) and the tails composed of refractory cells (marked by small points) after 99 time steps. If connection ties

(the weights) between the cells in the grid are strong ($w = 0.95$, $\Delta^* = 0.6$), excitation propagates uniformly outwards along four directions determined by geometry of the grid and the excitation line S (Fig. 3a). Wave propagation speed in all direction is the same. Strict geometry of the wave is being kept. No curvature effect is observed. In a mid of the excitation line, we have two planar waves that propagate upwards and downwards. If the connection ties between the cells in

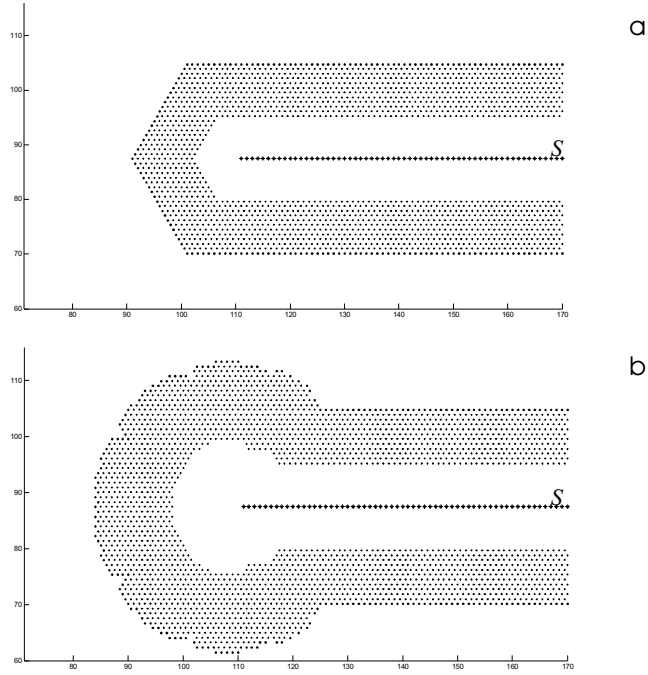


Fig. 3. Demonstration of curvature effect in isotropic hexagonal grid when a line of cells (S) was excited: a) $w = 0.95$, $t_{\text{refr}} = 54$, $\Delta^* = 0.6$; b) $w = 0.72$, $t_{\text{refr}} = 54$, $\Delta^* = 0.3$ ($m = 6$).

the grid are weaker ($w = 0.72$, $\Delta^* = 0.3$), the differences in excitation time of the cells appear. Differences in the excitation time shatter strict geometry of the wave (Fig. 3b). In such circumstances, weak ties between the cells are “broken”. Variations of wave propagation speed cause small clefts in the wave’s front. Even in homogeneous and isotropic grid we obtain speedy almost *radial wave propagation*. Two planar waves propagate upwards and downwards from

the mid of the excitation line approximately 1.5 times slower and have the same velocity as in the example 3a with $w = 0.95$.

3.2 Angular spread of the excitation

More details of radial wave propagation are explained in Fig. 4. In Fig. 4 we see

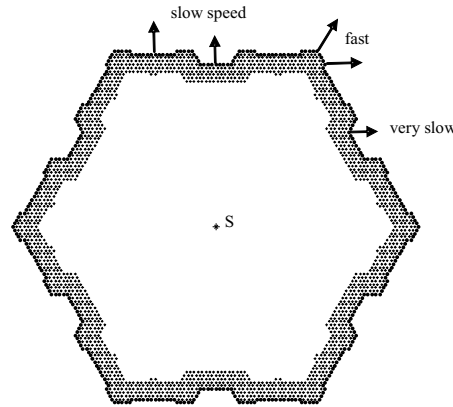


Fig. 4. Wave after $t = 208$ time moments in isotropic hexagonal grid when central cell (S) was excited ($w = 0.9$, $\Delta^* = 0.6$, $t_{\text{refr}} = 24$, $m = 6$). Wave propagation speed depends on local configuration of the wave.

a wave after $t = 208$ propagation steps in isotropic hexagonal grid with rather strong weights (connection strengths between the grid's elements) when central cell, S , was excited ($w = 0.9$, $\Delta^* = 0.6$). Large weights, w , resist the “tension due differences in wave propagation speed” and are trying to maintain the strict geometry of the wave. In six angles of the wave caused by hexagonal structure of the grid, the wave has a tendency to move outwards quicker as in the middle between two adjacent corners. In an example of Fig. 3a, a little bit stronger weights ($w = 0.95$) succeeded to keep the geometry strict. In present example, however, the weaker weights ($w = 0.9$) cannot resist the tensions due to the differences in the wave propagation speed. Continuous character of the cells' outputs generates numerous cell excitation patterns that occur in front of the wave. The variations in cells' excitation strengths cause different wave propagation speed. The wave front is breaking from time to time. In Fig. 4 we see multiple breaks. If refractory

period is small, the break of the front can cause gradually deepening cleft in the wave. The cleft helps the wave excitation to penetrate backwards, behind the wave and trigger daughter wavelets. In such situations, instead of “broken ring-fence of a castle” shaped wave we obtain beautiful “snowflakes”, “gearwheels”, etc.

3.3 Two mechanisms of “omega” wavelets

In case of small and moderate weights, we have multiple clefts. Therefore, we obtain almost radial wave propagation outwards of the starting cell. If refractory period is sufficiently short, we have gradually deepening cleft. Excitation penetrates backwards and triggers spontaneous burst of a secondary wave.

Fig. 5abc illustrates three early moments of this phenomenon. Arrow A in Fig. 5a points to small cleft in the wave’s front. Arrow B points to a single excited cell inside of the refractory cells behind the front of the wave. Arrow in

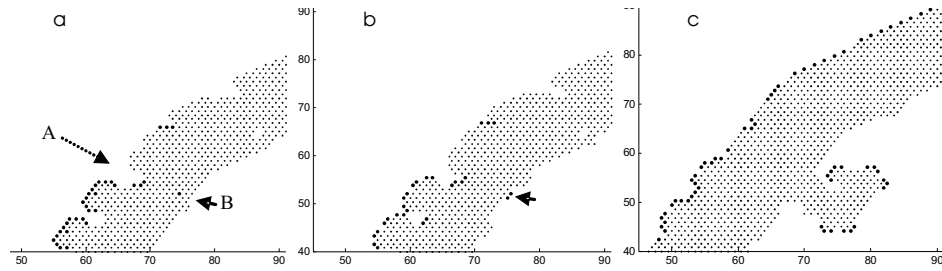


Fig. 5. The wave breakup and daughter wave initiation in isotropic hexagonal grid with weak connection weights between the cells ($w = 0.729$, $\Delta^* = 0.3$, $t_{\text{refr}} = 54$, $m = 6$): a) the wave after $t = 312$ time steps, b) $t = 316$; c) $t = 343$.

Fig. 5b indicates two excited cells that peer behind the refractory cells. Excitation spreads forwards and to both sides of the excitation stem. New wavelet (Fig. 5c) is composed of a pair of mirror-image spiral waves and reminds letter “ ω ” or a “mushroom of the smoke” one observes after an explosion of a powerful bombe. Therefore, we will call it “an omega wavelet”. Fig. 5c shows that in the daughter wave, the cells’ excitations propagate backwards up and down. In one of the simulation studies, we considered the models where signals of the cells excitation signals during two time moments were accumulated. In such models, we observed

more smooth symmetric patterns of the omega wavelets.

In further wave development, both spiral of the letter “ ω ” shaped wavelet contact, annihilate each other and instigates another cleft. The new cleft triggers one more omega wavelet, e.t.c. Simulations show that irrespective to the lengths of refractory period, this part of excitable media becomes a pacemaker. The wavelet generation period mainly is determined by refractory period of the media.

3.4 The wave’s breakup

The information transmission model suggests two cleft birth mechanisms that cause wave breakup. First of them is based on gradually deepening clefts in the wave caused by uneven propagation speed of curved and planar segments of the wave and short refractory period. The second one is based on the shape of the omega wavelet composed of two spirals. In both cases, the clefts facilitate the excitation signal penetrate through layer of refractory cells and initiate the daughter wavelets.

At boundaries of the grid, the cells are connected to smaller number of adjacent ones. Therefore, after colliding with the boundaries the waves vanish. If the omega wavelet emerges close to the boundary of the grid, the boundary can put out one part of the spiral. In such case, we obtain one armed spiral. In Fig. 6a we have spiral wave started by the cleft in original wave in a vicinity of the left bottom edge of the grid. In figure we see: original wave, O, triggered by excitation of a single cell close to left bottom corner of the grid, two loops of secondary spiral wave, A, instigated by the cleft in wave’s O front near the bottom edge of the grid. In Fig. 6a we see also the third spiral (wave B, three loops in left bottom corner of the grid). This wave was initiated by the cleft in front of the second loop of wave A. At the very edge of the left border, we observe a birth of fourth spiral, C. Later the fronts of the wavelets’ are breaking further producing fragmentation and complicating the activation pattern. The region of chaotic behavior gradually extends to the whole medium, leading to complex patterns composed of many wavelets of various sizes (Fig. 6b). The analysis hints that the wave breakdown and the daughter wavelet bursting behavior possibly is inherent peculiarity of excitable media with weak ties between the cells, direct dependence of the signal transmission time on the cell’s output, the short refractory period and granular

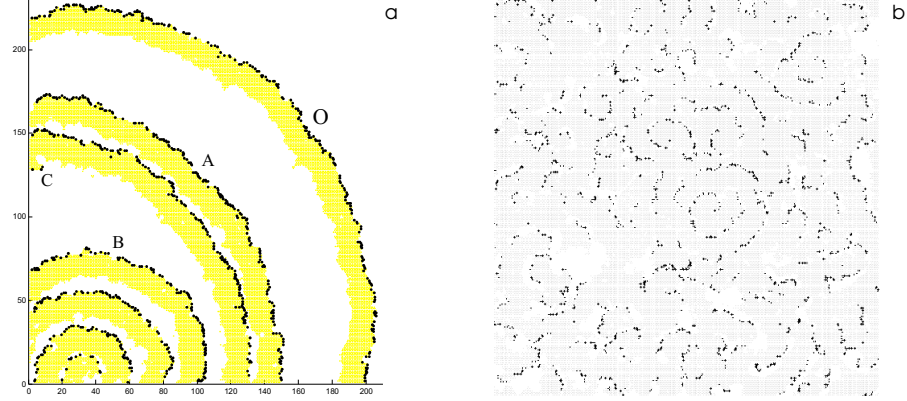


Fig. 6. a) – a wave after $t = 312$ time steps initiated by initial wave breaks close to the edges of isotropic hexagonal grid; weak connection ties between the cells ($w = 0.6$, $\Delta^* = 0.1$, $t_{\text{refr}} = 28$, $m = 6$): O – original wave initiated by excitation of single cell close to left bottom corner of the grid, A – two waves of secondary spiral that initiated third spiral wave B (three loops in left bottom corner of the grid); C – birth of fourth spiral on edge of left border of the grid; b) – development of Fig. 6a – the wave after $t = 3380$ time steps: spontaneous wave initiations at borders and inside the grid, their meandering and break-down.

structure.

4 Discussion

New cellular model of excitable media with continuous outputs and varying cells' excitation time was proposed. The model suggested gives insights concerning the spiral wave formation in isotropic homogeneous excitable media. In analysis of the wave birth, propagation and destruction, we think basically in terms of information. *It is the information that is important, regardless of the manner in which it is acquired.* Therefore, the single layer perceptrons were utilized to simulate information transmission from of one element of the grid to other ones. Contrary to known cellular automaton models of excitable media with discrete outputs of the cells, in the new model we have continuous outputs. This factor produces countless number of local excitation patterns in front of the wave. Infinitesimal calculation inaccuracies initiate minute differences and can trigger

spiral waves and produce chaotic wave propagation in the media. Our research allows guess that bursting behavior caused by minuscule inaccuracies and local differences in wave propagation speed is inherent peculiarity of excitable media with weak ties between the cells, short refractory period and cellular structure.

In our research we performed hundreds of wave propagation studies with 1D, 2D and 3D hexagonal or rectangular grids, randomized them by adding random shifts, size of the grid, considered various shapes of obstacles, constant and variable refractory periods, different characters of activation function, $f(arg)$, sets of parameters $w_1, w_2, \dots, w_p, \Delta^*, m, p, arg_{start}$, e.t.c. We found that larger size of the grid creates more variants and higher probability that occasional clefts in the wave front will permit the excitation signal to penetrate behind the refractory cells.

When w is large and m is small, our model degenerates to simple CA model with discrete valued outputs where only one cell is sufficient to excite another neighboring cell. We see that like in artificial neural network analysis of pattern recognition and prediction algorithms, investigation of aging phenomena in chaotically changing environments [31]–[35], in the excitable media research, *the magnitudes of the weights are of primary importance*. Strong ties between the elements of the grid make the waves propagation patterns as a subtle crystal. Possibly, new model could be useful in crystallography. Diminution of weights causes occasional clefts if front of the wave and makes the wave pattern radial. If refractory period is small, spontaneous wave birth can be observed. Such situations are more characteristic to plasma physics, biology, meteorology, etc. Usually an increase in connection weights, w , requires simultaneous increase in Δ^* . Particular character of the waves is determined by combination of parameters $w_1, w_2, \dots, w_p, \Delta^*, m, t_{refr}, p, arg_{start}$. Above arguments advocate that *continuous outputs of the cells in the model and varying cells' excitation time introduce a new quality*.

The contribution of the new information transmission concept based model is two-fold. First, it gives a new tool to model excitable media behavior in applied disciplines such as physics, biology and social sciences. Second, it is a new line of attack aimed to understand wave bursting, propagation and annihilation processes. Together with differential equations based and CA approaches it can reveal new,

so far unidentified peculiarities of the excitable media.

The new model is located between cellular automaton with discrete outputs and differential equation based models. The differential equation based models possibly are too “precise” and do not reflect cellular structure of the abundance of real excitable medias. The CA based models work in discrete cells’ outputs space and also do not point to birth of the clefts in front of the propagating wave [2, 37]. The model with continuous outputs succeeds to come across the clefts problem and explain radial character of the wave propagation in strictly hexagonal grid, spontaneous birth of daughter wavelets, e.t.c. From the point of view of calculation speed, the new model stands between cellular automaton based on the set of rules that determine future states of the cells in the grid and the CA models based on coupled differential or difference equations used to simulate the behavior of the single cell.

References

1. Bub G., Shrier A. “Propagation through heterogeneous substrates in simple excitable media models”, *Chaos*, **12**(3), p. 747–753, 2002
2. Bub G. *Optical Mapping of Pacemaker Interactions*. Ph.D. thesis, McGill Univ., Dept. Physiology, Montreal, Canada, 2000
3. Field R.J., Burger M. (Eds.) *Oscillations and Traveling Waves in Chemical Systems*, Wiley and Sons, New York, 1985
4. Winfree A.T. “Rotating chemical reactions”, *Scientific American*, **230**(12), p. 82–85, 1974
5. Winfree A.T. “Wave propagation in cardiac muscle and in nerve networks”, In: *Handbook of Brain Theory and Neural Networks*, Arbib M., (Ed.), p. 1054–1056, 1995
6. Wiener N., Rosenblueth A. “The mathematical formulation of the problem of conduction of impulses in a network of connected excitable elements, specifically in cardiac muscle”, *Arch. Ins. Cardiol. Mex.*, **16**, p. 205–265, 1946
7. Allesie M.A., M. Bonke F.I., Schopman F.J.G. “Circus movement in rabbit atrial muscle as a mechanism of tachycardia: III The leading circle”, *Circulation Research*, **41**, p. 9–18, 1977
8. Vinson M., Mironov S., Mulvey S., Pertsov A. “Control of spatial orientation and lifetime of scroll rings in excitable media”, *Nature*, **388**(3), p. 477–480, 1997

9. Henriquez C.S., Papazoglou A.A. "Using computer models to understand the roles of tissue structure and membrane dynamics in arrhythmogenesis", In: *Proceedings of the IEEE*, **84**(3), p. 334–354, 1996
10. Hodgkin A.L., Huxley A.F. "A quantitative description of membrane current and its application to conduction and excitation in nerve", *Journal of Physiology*, **117**, p. 500–544, London, 1952
11. Gerhardt M., Schuster H., Tyson J.J. "A cellular automaton model of excitable media including curvature and dispersion", *Science*, **247**, p. 1563–1566, 1990
12. Farley B.G. *Computers in Biomed. Res.*, **1**, p. 265–294, 1965
13. Moe G.K., Rheinbolt W.C., Abildskov J.A. "A computer model of atrial fibrillation", *Am. Heart J.*, **67**, p. 200–220, 1964
14. Balakhovskij I.S. "Several modes of excitation movement in ideal excitable tissue", *Biophysika*, **10**, p. 1175–1179, 1965
15. Krinsky V.I. "Spread of excitation in an inhomogeneous medium (state similar to cardiac fibrillation)", *Biophysika*, **11**, p. 776–784, 1966
16. Greenberg J.M., Hastings S.P. "Spatial patterns for discrete models of diffusion in excitable media", *SIAM J. Applied Mathematics*, **34**, p. 515–523, 1978
17. Gerhardt M., Schuster H., Tyson J.J. "Cellular automaton model of excitable media II. Curvature, dispersion, rotating waves and meandering waves", *Physica D*, **46**(3), p. 392–415, 1990
18. Marcus M., Hess B. "Isotropic cellular automaton for modeling excitable media", *Science*, **347**, p. 56–58, 1990
19. Kurrer C., Schulten K. "Propagation of chemical waves in discrete excitable media: anisotropic and isotropic wave fronts", In: *Nonlinear Wave Processes in Excitable Media*, Holden A.V., Markus M., Othmar H.G., (Eds.), Plenum Press, New York, p. 489–500, 1991
20. Gerhardt M., Schuster H., Tyson J.J. "A cellular automaton model of excitable media III. Fitting the Belousov-Zhaboinski reaction", *Physica D*, **46**(3), p. 416–426, 1990
21. Weimar J., Tyson J.J., Watson L.T. "Diffusion and wave propagation in cellular automaton models of excitable media", *Physica D*, **55**, p. 309–327, 1992
22. Tyson J.J., Keener J.P. "Singular perturbation theory of traveling waves in excitable media: a review", *Physica D*, **32**, p. 327–361, 1988

23. Christini D.J., Glass L. "Mapping and control of complex cardiac arrhythmias", *Chaos*, **12**, p. 732–739, 2002
24. Krinsky V.I. *Problemy Kibernetiky*, **20**, p. 59–80, 1968
25. Winfree A.T. "Electrical instability in cardiac muscle: Phase singularities and rotors", *J. Theor. Biology*, **138**, p. 353–405, 1989
26. Palsson E., Cox E.C. "Origin and evolution of circular waves and spirals in Dictyostelium discoideum territories", In: *Proc. Natl. Acad. Sci. USA*, **93**, p. 1151–1155, 1996
27. Davidenko J.M., Kent P.F., Chialvo D.R., Michales D.C., Jalife J. "Sustained vortex-like waves in normal isolated ventricular muscle", In: *Proc. Natl. Acad. Sci. USA*, **87**, p. 8785–8789, 1990
28. Fenton F.H., Cherry E.M., Hastings H.M., Evans S.J. "Multiple mechanisms of spiral wave break", *Chaos*, **12**, p. 852–892, 2002
29. Panfilov A., Pertsov A. "Ventricular fibrillation: evolution of the multiple-wavelet hypothesis", *Phil. Trans. R. Soc. London*, **359A**, p. 1315–1325, 2001
30. Haykin S. *Neural Networks: A comprehensive foundation* (2nd edition), Macmillan College Publishing Company, Inc., New York, 1998
31. Raudys S. "On the universality of the single-layer perceptron model", In: *Neural Networks and Soft Computing*, Rutkowski L., Kacprzyk J. (Eds.), Physica & Springer-Verlag, NY, p. 79–86, 2003
32. Raudys S. "Evolution and generalization of a single neurone. I. SLP as seven statistical classifiers", *Neural Networks*, **11**(2), p. 283–296, 1998
33. Raudys S. *Statistical and Neural Classifiers: an integrated approach to design*, Springer, London 2001
34. Raudys S. "Evolution and generalization of a single neurone. III. Primitive, regularized, standard, robust and minimax regressions", *Neural Networks*, **13**(3/4), p. 507–523, 2000
35. Raudys S. "An adaptation model for biological and social aging", *Int. J. of Modern Physics*, **13**(8), p. 1075–1086, 2002
36. Spach M.S. "Discontinuous cardiac conduction: its origin in cellular connectivity with long-term adaptive changes that cause arrhythmias", In: *Discontinuous Conduction in the Heart*, Spooner P.M., Joyes R.W., Jalife J. (Eds.), Futura Publ. Company, Inc., Armonk, NY, p. 5–51, 1997
37. Kleber A.G., Rudy Y. "Basic mechanisms of cardiac impulse propagation and associated arrhythmias", *Physiological reviews*, **84**(2), p. 431–488, 2004